Biochimica et Biophysica Acta 1807 (2011) 1114–1124

Contents lists available at ScienceDirect

Biochimica et Biophysica Acta

journal homepage: www.elsevier.com/locate/bbabio

# Variation of flux control coefficient of cytochrome c oxidase and of the other respiratory chain complexes at different values of protonmotive force occurs by a threshold mechanism

Giovanni Quarato [1], Claudia Piccoli, Rosella Scrima, Nazzareno Capitanio *

*Department of Biomedical Sciences, University of Foggia, Foggia, Italy*

ARTICLE INFO

*Article history:*
Received 21 January 2011
Received in revised form 10 April 2011
Accepted 13 April 2011
Available online 1 May 2011

*Keywords:*
Metabolic control analysis
Oxidative phosphorylation
Mitochondrial membrane potential
Cytochrome c oxidase
Respiratory chain supercomplexes

ABSTRACT

The metabolic control analysis was applied to digitonin-permeabilized HepG2 cell line to assess the flux control exerted by cytochrome c oxidase on the mitochondrial respiration. Experimental conditions eliciting different energy/respiratory states in mitochondria were settled. The results obtained show that the mitochondrial electrochemical potential accompanies a depressing effect on the control coefficient exhibited by the cytochrome c oxidase. Both the components of the protonmotive force, i.e. the voltage ($\Delta\Psi_m$) and the proton ($\Delta pH_m$) gradient, displayed a similar effect. Quantitative estimation of the $\Delta\Psi_m$ unveiled that the voltage-dependent effect on the control coefficient of cytochrome c oxidase takes place sharply in a narrow range of membrane potential from 170–180 to 200–210 mV consistent with the physiologic transition from state 3 to state 4 of respiration. Extension of the metabolic flux control analysis to the NADH dehydrogenase and $bc_1$ complexes of the mitochondrial respiratory chain resulted in a similar effect. A mechanistic model is put forward whereby the respiratory chain complexes are proposed to exist in a voltage-mediated threshold-controlled dynamic equilibrium between supercomplexed and isolated states.



## 1. Introduction

Mitochondrial respiration constitutes the main process sustaining cell bioenergetic. It is accomplished by respiratory chain (RC) complexes which transfer reducing equivalents from NADH or flavin-containing enzymes ultimately to oxygen. The redox-driven proton pumping activities of complexes I, III and IV and the protonmotive-driven $H^+$-FoF1 ATP synthase provide the coupling mechanism for the oxidative phosphorylation (OXPHOS) [1].

The identification of the step(s) controlling cell respiration has been the object of a number of studies which recently exploited the theoretical framework of the metabolic control analysis (MCA) [2–4]. A fundamental concept of MCA is the control coefficient ($C^J_{v,i}$), which gives a measure of the sensitivity of a systemic variable to a particular parameter. Accordingly, in a pathway of reactions sequentially catalyzed by a series of enzymes the control exerted on the overall flux depends mainly on the step(s) exhibiting the higher values in the $C^J_{v,i}$(s). Conversely, a step with a low $C^J_{v,i}$ can scarcely influence the global flux even when its amount is drastically reduced. For this reason, it is important to define the specific control strength exerted by a given enzymatic step and the threshold level beyond which a deficit in the content of that enzyme starts to become functionally limiting [5,6].

The rate of cell respiration is largely controlled by the rate of the electron transfer through the mitochondrial RC [7] which is feed-back modulated by the extent of the protonmotive force/electrochemical membrane potential ($\Delta\mu_{H+}$) [1]. The latter is in turn controlled by the rate of the ATP synthesis and by other $\Delta\mu_{H+}$-dissipative systems. However, which specific step within the composite RC owns the main control strength over the global electron transfer as well as the actual value of the $C^J_{v,i}$(s) is less defined. The reasons of the controversial results so far reported partly depend on the biological sample used. MCA on isolated mitochondria gives rise to different $C^J_{v,i}$s for components of the RC as compared with similar analysis carried out on in situ mitochondria (i.e. intact or cell-membrane permeabilized cells) [8]. Furthermore, the energy state of the mitochondrial membrane is emerging as a potential factor influencing the respiratory flux control exerted by a given RC complex [9,10].

*Abbreviations:* MCA, metabolic control analysis; GRF, glogal respiratory flux; COX-IS, cytochrome c oxidase isolated enzymatic step; $C^J_{v,COX}$, flux control coefficient of COX; $C^J_{v,CI}$, flux control coefficient of complex I; RC, respiratory chain; COX, cytochrome c oxidase; $\Delta\mu_{H+}$, mitochondrial transmembrane electrochemical proton gradient; $\Delta\Psi_m$, mitochondrial transmembrane electrical potential; $\Delta pH_m$, mitochondrial transmembrane pH gradient; OXPHOS, oxidative phosphorylation; FCCP, carbonyl-cyanide p-trifluoromethoxyphenylhydrazone; TMRE, tetramethylrhodamine, ethyl ester; UQ, ubiquinone; ROS, reactive oxygen species

* Corresponding author at: Department of Biomedical Sciences, University of Foggia, via L. Pinto OO.RR., 71100, Foggia, Italy. Tel.: +39 0881 711148; fax: +39 0881 714745.
*E-mail addresses:* quarato@sciences.sdsu.edu (G. Quarato), n.cap@unifg.it (N. Capitanio).
[1] Present address: BioScience Center, San Diego State University, 5500 Campanile Drive, San Diego, CA 92182-4650.

0005-2728/$ – see front matter © 2011 Elsevier B.V. All rights reserved.
doi:10.1016/j.bbabio.2011.04.001

In this study we extended previous MCA-related observations on endogenously respiring intact cells [9] to address the following specific points: a) to confirm the impact of the mitochondrial membrane energy state on the respiratory flux control of cytochrome c oxidase ($C^J_{v,COX}$) in digitonin-permeabilized cells under more controlled OXPHOS-substrate delivery; b) to assess the specific effect of the two components of the mitochondrial transmembrane electrochemical potential ($\Delta\mu_{H+}$), the voltage ($\Delta\Psi_m$) and the proton ($\Delta pH_m$) gradients; and c) to define on a quantitative basis the relationship between the $\Delta\Psi_m$ and the $C^J_{v,COX}$.

## 2. Materials and methods

### 2.1. Cell cultures

Human hepatoma-derived cell line (HepG2), normal human dermal fibroblasts (NDHF) and murine myoblast cell line (L6) were grown in DMEM (Dulbecco's modified Eagle's medium) supplemented with 10% (v/v) fetal bovine serum to 70–80% confluence before harvesting. Cells were detached from 150 mm-diameter Petri dishes with 2 ml of 0.05% trypsin/0.02% EDTA and washed in 20 ml of phosphate buffer saline (PBS), pH 7.4, with 5% (v/v) calf serum, centrifuged at 500×*g*, re-suspended in 200 μl of PBS, counted and immediately used. Cell viability, as determined by Trypan Blue exclusion, was typically never below 98%.

### 2.2. Polarographic measurements

The rate of oxygen consumption was measured by high-resolution oxymetry (Oxygraph-2k, Oroboros Instruments) with a Clark-type oxygen electrode in a thermostatically controlled chamber equipped with a magnetic stirring device and a gas-tight stopper fitted with a narrow port for additions via Hamilton micro-syringes. Measurements were carried out at 37 °C with 1–2×$10^6$ HepG2 cells/ml suspended in 0.25 mM sucrose, 10 mM $KH_2PO_4$, 27 mM KCl, 40 mM Hepes, 1 mM $MgCl_2$, 0.5 mM EGTA, 0.1% BSA, pH 7.1 supplemented with 20 μg digitonin/ml/$10^6$ cells. The minimal amount of digitonin suppressing cell respiration (in the presence of oligomycin) but resulting in recovery of the activity following addition of pyruvate + malate and in a respiratory control ratio ≥8 in the presence of FCCP was chosen. When indicated 1 mM ADP, 0.8 μM carbonylcyanide p-trifluoromethoxyphenylhydrazone (FCCP), 35 nM nigericin, 45 nM valinomycin were added (singularly or in combination) to the assay medium. The minimal concentrations of nigericin and valinomycin eliciting the maximal increase and collapse of the $\Delta\Psi_m$ respectively (see below) were selected. Oxygen consumption for the global respiration flux (GRF) was sustained by 2 mM pyruvate + 2 mM malate ± 2 mM succinate; oxygen consumption by COX as isolated step (COX-IS) by 10 mM ascorbate + 0.2 mM TMPD in the presence of 0.2 μM antimycin A + 1 μM rotenone. Higher concentrations of TMPD enhanced the COX-IS activity but resulted also in a high residual CN-insensitive $O_2$-consumption likely due to auto-oxidation of TMPD. Inhibitory titrations of the respiratory activities were performed by sequential additions of 0.5–1.0 μl of freshly prepared concentrated solutions of KCN, antimycin A, rotenone.

### 2.3. Metabolic control analysis (MCA)

The respiratory flux control coefficient of COX ($C^J_{v,COX}$) was estimated from the ratio of the initial slopes of the KCN titration/inhibition curves of the GRF and COX IS (graphic method) [3]. Alternatively, the $C^J_{v,COX}$ was calculated from a non linear regression analysis of the inhibitor-titration data set as developed in [11, see also 12] and modified in [9] (fitting method). The derived non-linear equation correlating the percentage of the GRF to the inhibitor concentration depends on three parameters: $K_D$, which is the dissociation constant of the EI complex, $E_0$, which is the total amount of the active enzyme (i.e. COX), and $C^J_{v,i}$, which is the control coefficient of the inhibited enzymatic step. Kd was estimated by Dixon plot analysis of the COX IS (in the presence of 0.8 μM FCCP) resulting in 25 ± 5 μM (n = 15). The content of COX was evaluated by the dithionite-reduced minus air-oxidized differential spectra of HepG2 cell lysate resulting 4.8 ± 0.5 pmol $aa_3$/$10^6$ cells (n = 5; $\Delta\varepsilon_{650-630nm} = 24\ mM^{-1}\ cm^{-1}$) and thus a value for $E_0 = 0.005$ μM was assumed at the prevailing experimental conditions (i.e. at $10^6$ HepG2 cells/ml). The parameter $C^J_{v,COX}$, was estimated by best-fitting the inhibitory titration data set using the program GraFit 4.0.13 (Erithacus Software Ltd., Horley, Surrey, U.K.). The accuracy of the fitting method was further tested as in [9].

### 2.4. Measurement of the mitochondrial transmembrane potential ($\Delta\Psi_m$)

The $\Delta\Psi_m$ was assessed spectrofluorimetrically with safranine O [13,14]. HepG2 cells were suspended at $10^6$ cells/ml in the respiration-assay medium eventually supplemented with ADP and/or ionophores at the concentrations detailed in the previous section. After 10 min of incubation with digitonin the cell suspension was transferred to the spectrofluorimetric cuvette equipped with a thermostatic control system (T = 37 °C) and a stirring device. The instrumental setting was $\lambda_{ex} = 495$ nm, $\lambda_{em} = 596$ nm, medium gain (FP-6500, Jasco Analytical Instruments). The fluorescence signal was calibrated by four consecutive additions of 2.5 μM safranine O and the respiratory activity started by addition of 2 mM pyruvate + 2 mM malate. To calculate the $\Delta\Psi_m$, the fluorescence signal was first converted in concentration of safranine O using a non linear fitting equation of the calibrated fluorescence signals and then the changes in safranine O concentrations were converted to mV using the Nernst equation: $\Delta\Psi_m(mV) = 60 \cdot \log_{10}[S]_{in}/[S]_{out}$; with $[S]_{in}$ and $[S]_{out}$ standing for intramitochondrial and extramitochondrial concentration of safranine O respectively. The intramitochondrial volume was estimated on an average basis to amount to ≈50% of the total HepG2 cell volume by stereological analysis of confocal microscopy imaging of the tetramethylrhodamine, ethyl ester (TMRE) distribution (see also [15,16]). Estimation of the total cell volume resulted in ≈6 pl/cell thus an intramitochondrial volume of 3 μl/$10^6$ cells was used (see also biometric parameters in http://bionumbers.hms.harvard.edu/). No correction for bound safranine O was applied because titration of the fluorescence signal with the dye in buffer without or with cells (in the absence of respiratory substrates and in the presence of 3 μM FCCP) resulted in undistinguishable calibration curves.

### 2.5. Statistical analyses

The two-tailed Student's *t*-test was applied, with a $P<0.05$, to evaluate the statistical significance of differences measured throughout the data sets presented.

## 3. Results

### 3.1. The respiratory flux control of COX depends on the membrane energization state in permeabilized cells and on the combination of the respiratory substrates

In a previous MCA study in intact HepG2 cells we reported that the $C^J_{v,COX}$ exhibited a high value under resting (phosphorylating) endogenous respiration and was negatively regulated under conditions preserving dissipation of the $\Delta\mu_{H+}$ (i.e. in the presence of oligomycin [9]). Similar results were obtained in intact murine myoblasts (L6) cell line and primary normal human dermal fibroblasts (NDHF) (supplementary Fig. S1) thereby confirming that the depressing effect of the mitochondrial $\Delta\mu_{H+}$ on the $C^J_{v,COX}$ was a general phenomenon irrespective of the cell phenotypical background.

To consolidate this finding we extended the MCA to digitonin-permeabilized HepG2 cells. By high resolution oxymetry the results of the KCN titration on the activity of the mitochondrial RC-dependent global respiratory flux (GRF) sustained by exogenous additions of pyruvate plus malate (P/M) and on the COX isolated step (COX-IS) by ascorbate plus TMPD were analyzed. The KCN titrations were carried out both in the absence and in the presence of ADP (i.e. respiratory state $4_{-\,ADP}$ and $3_{+\,ADP}$ as defined in [17]). The GRF under state $4_{-\,ADP}$ resulted in a significant resistance to KCN inhibition as compared to that of state $3_{+\,ADP}$. The respiratory state-dependent sensitivity to KCN was practically absent in the COX-IS (see supplemental Fig. S2). Plots of the percentages of inhibition of the GRF and the COX-IS (Fig. 1A) enabled estimation of the $C^{J}_{v,COX}$ which resulted in $0.056 \pm 0.017$ under state $4_{-\,ADP}$ and $0.261 \pm 0.046$ ($P<0.001$) under state

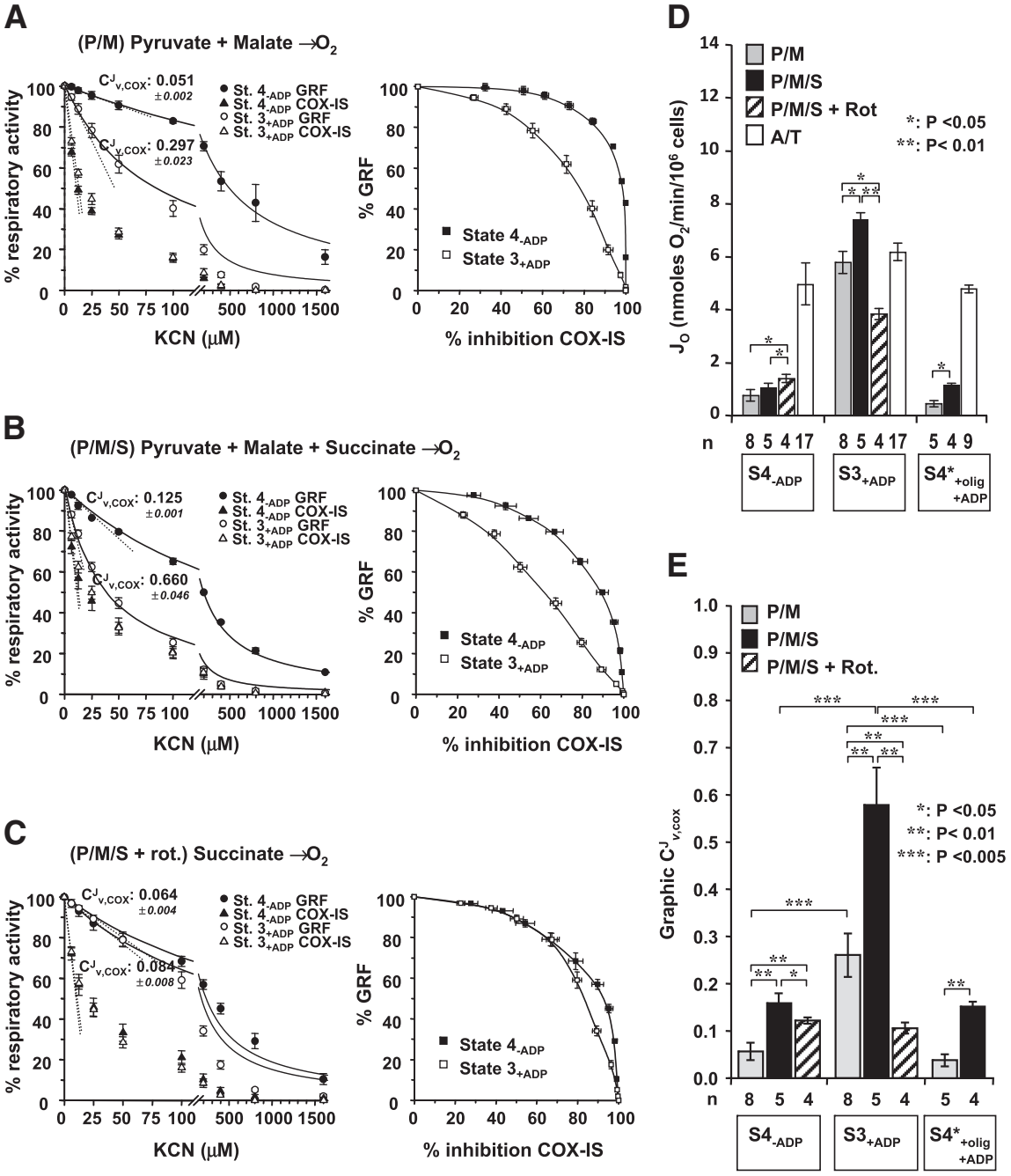


**Fig. 1.** Inhibitory KCN titrations analysis of the respiratory activities in digitonin-permeabilized HepG2 cells. Panels A–C, KCN titration of the GRF and COX-IS. The respiratory substrates sustaining the GRF were 2 mM pyruvate + 2 mM malate (P/M, panel A), pyruvate + malate + 2 mM succinate (P/M/S, panel B), pyruvate + malate + succinate in the presence of 1 μM rotenone (P/M/S/ + rot, panel C) and 10 mM ascorbate + 0.2 mM TMPD (A/T) for the COX-IS. The closed and open symbols refer to the respiratory states $4_{-\,ADP}$ and $3_{+\,ADP}$ (in the presence of 1 mM ADP) respectively (as indicated in the symbol legends) and are means ± s.e.m. of $n \geq 4$ independent cell preparations. The split x axis enlarges the low concentration range of the inhibitor wherefrom the $C^{J}_{v,COX}$s were graphically estimated from the ratio of the slopes obtained by linear regression analysis of the first 3–4 titration points (indicated as dotted lines) and shown in panel E. The continuous lines are a non-linear regression best fit applied to the data points of the GRF whereby the indicated $C^{J}_{v,COX}$s were estimated from the parametric equation described in the Materials and Methods section. The graphs on the right of each panel are the threshold plot representations derived from the respective KCN inhibitory profiles. Panel D, uninhibited oxygen consumption rates of the GRF and COX-IS. When indicated ADP ± 1.26 μM oligomycin, was present in the assay medium. Each bar indicates the mean value ± s.e.m. of the indicated *n* independent cell preparations along with the statistical analysis of the differences when significant. The GRFs under $S4_{-\,ADP}$ and $S4^{*}_{+\,ADP\,+\,olig}$ resulted in no significant difference whereas both exhibited a $P<0.0001$ when compared to $S3_{+\,ADP}$. Panel E, $C^{J}_{v,COX}$s measured by the "graphic" method. The statistical analysis between group-related pairs of $C^{J}_{v,COX}$ values is shown when the difference was significant.

$3_{+ADP}$ (estimated by graphic method, Fig. 1E). Importantly similar results were obtained when the $C^J_{v,COX}$ was assessed by non-linear regression analysis of the sole GRF inhibition [11] ($0.051 \pm 0.001$ and $0.297 \pm 0.022$ in state $4_{-ADP}$ and $3_{+ADP}$ respectively).

The respiratory control ratio of the uninhibited GRF activities (i.e. state $3_{+ADP}$/state $4_{-ADP}$) was >8 indicating a full competence of the mitochondria in digitonin-permeabilized cells in maintaining a high protonmotive force.

The threshold plot provided further evidence of the effect of the membrane energy state on the apparent control strength/reserve capacity of COX (Fig. 1A). In state $3_{+ADP}$ a 60% decrease of the IS resulted in about 30% inhibition of the GRF whereas in state $4_{-ADP}$ a 60% decrease of the IS resulted in about 5% inhibition of the GRF.

Transfer of reducing equivalents to both complexes I and II, achieved by succinate along with pyruvate plus malate (P/M/S), resulted in a higher sensitivity to KCN and in a higher $C^J_{v,COX}$ both in state $3_{+ADP}$ and $4_{-ADP}$ ($0.660 \pm 0.048$ and $0.125 \pm 0.001$ respectively, Fig. 1B,E). The threshold plot, in the presence of succinate, confirmed the effect accompanying the membrane energy state on the $C^J_{v,COX}$ in a manner more closely resembling that observed in intact cells (cf. the threshold plots of Figs. 1B and S1A). Intriguingly, when the KCN titration was carried out with P/M/S but in the presence of rotenone (thus setting conditions for electron transfer occurring only via complex II) the effect of the respiratory state on the COX-mediated control vanished with a $C^J_{v,COX}<0.1$ both in state $4_{-ADP}$ and state $3_{+ADP}$ (Fig. 1C,E).

In the presence of ADP plus oligomycin (state $4^*_{+ADP/olig}$) both the GRF rates and the $C^J_{v,COX}$s were significantly depressed as compared to state $3_{+ADP}$ (Fig. 1D,E). This observation ruled out any involvement of ADP in the differential effect of the membrane energy state on the $C^J_{v,COX}$.

### 3.2. The two components of the $\Delta\mu_{H+}$, $\Delta\Psi_m$ and $\Delta pH_m$, exhibit a similar effect on the COX-mediated respiratory flux control

Since the $\Delta\mu_{H+}$ generated by the mitochondrial RC comprises a voltage and a pH gradient [1] we wondered whether these two thermodynamic components had comparable or differential effects on the $C^J_{v,COX}$. To this aim we performed the MCA in the presence of either the $K^+/H^+$ exchanger nigericin and the $K^+$-ionophore valinomycin to maximize the contribution of the $\Delta\Psi_m$ or the $\Delta pH_m$ to the $\Delta\mu_{H+}$ [1]. In addition, the effect of the protonophoric uncoupler FCCP was tested.

Fig. 2A shows that when compared with state(s) 4 either valinomycin or FCCP caused a significant enhancement of the P/M-, P/M/S- and A/T-dependent oxygen consumption (more pronounced in the GRF) whereas nigericin did not cause significant changes (cf. Figs. 1D and 2C). The MCA resulted in the following outcomes: i) in the presence of nigericin the $C^J_{v,COX}$ was $0.013 \pm 0.003$ and $0.093 \pm 0.025$ for the P/M- and P/M/S-dependent respiration respectively and the corresponding threshold plots were further right-shifted as compared with those obtained under state $4_{-ADP}$ (cf. Figs. 1A,B and 2A); ii) in the presence of valinomycin the KCN titration curve displayed a lower inhibition comparable with that observed in the presence of nigericin, particularly at low concentrations of the inhibitor, whereby the $C^J_{v,COX}$ was $0.035 \pm 0.011$ and $0.088 \pm 0.011$ for the P/M- and P/M/S-dependent respiration respectively and the threshold plots presented an almost unchanged respiratory rate of the GRF up to 40% inhibition of the COX-IS; iii) in the presence of FCCP the titration with KCN resulted in a much less sigmoidal inhibitory curves with both the $C^J_{v,cox}$ and the threshold plots closely resembling those obtained under state $3_{+ADP}$.

When a similar analysis was carried out in the presence of ADP (without oligomycin) the addition of nigericin caused a significant depression of the GRFs with no apparent change in the COX-IS whereas addition of either valinomycin or FCCP resulted in a further enhancement of the oxygen consumption activities in both. Interestingly, the MCA unveiled that both nigericin and valinomycin caused a marked increase of the resistance to KCN as compared to what was observed under state $3_{+ADP}$ in the absence of ionophores. Consequently, this resulted in a relatively low $C^J_{v,COX}$ (Fig. 2D) and a right-shifted curve of the threshold plot. Conversely, addition of FCCP did not cause major changes in the $C^J_{v,COX}$ which resulted comparable with that attained under state $3_{+ADP}$.

It is worth noting that, the data in Fig. 2C,D show that the $C^J_{v,COX}$ was six-fold lower in the presence of valinomycin as compared to that attained with FCCP though the actual respiratory rates in both conditions were comparably higher with respect to the states $4_{-ADP}$ and $4_{+ADP/olig}$. In particular, the initial rate of the COX-IS in the presence of valinomycin was comparable with that of the P/M-dependent GRF and even lower than the P/M/S-dependent GRF at variance with what was observed under state 4 or in the presence of nigericin. All this, would rule out that the impact of the membrane energy state on the $C^J_{v,COX}$ was vitiated/biased by the actual velocity or elasticity of the COX-IS.

It must be pointed out that the binding of $CN^-$ takes place at the heme $a_3$ of COX in the ferric state [18,19]. A slow binding of $CN^-$ to the oxidized enzyme has been reported for the so called "resting" purified COX. However this limitation does not apply to our conditions since COX was continuously turning over and the binding of $CN^-$ was completed within the time-window of the measurements [18]. The steady-state reduction level of the COX redox centers is known to be affected by the membrane potential [1] and thus one could argue that the different "sensitivity" to the inhibitor might depend on the different oxidation state of the inhibitor-binding site. This concern does not apply to our case because heme $a_3$ is located downstreams of the $Cu_A$-heme *a* electrogenic step within the COX [20,21] therefore in the presence of a $\Delta\Psi_m$ heme $a_3$ is more oxidized than under membrane de-energized condition. If the different sensitivity to $CN^-$ between the respiratory states 4 and 3 depended on the redox state of heme $a_3$ one would expect a minor resistance under state 4 (i.e. high $\Delta\Psi_m$) which instead was the opposite of what was observed.

Collectively these observations suggested that conversion of the $\Delta\mu_{H+}$ in either $\Delta\Psi_m$ or $\Delta pH_m$ had a similar depressing impact on the control strength exerted by COX over the GRF and that collapse of the whole $\Delta\mu_{H+}$ did not result in significant changes of the $C^J_{v,COX}$ as compared to state $3_{+ADP}$.

### 3.3. A relatively small increase of the membrane potential accounts for the effect of the membrane energy state on COX-mediated respiratory flux control

To assess the reliability of our results we measured the $\Delta\Psi_m$ (the major component of the $\Delta\mu_{H+}$ [1]) in permeabilized HepG2 under the prevailing conditions used in the MCA utilizing the fluorescent probe safranine O in the P/M-"mode" of respiration (Fig. 3A). The calculated value of the $\Delta\Psi_m$ was, under state $4_{-ADP}$ of respiration, $193.6 \pm 1.5$ mV ($n = 10$) (Fig. 3B) closely matching the $\Delta\Psi_m$ value estimated under similar condition in isolated mitochondria using different methodological approaches [22]. Additions of KCN up to 50 μM did not cause significant change of the $\Delta\Psi_m$ which, however, progressively decreased at higher titers of the inhibitor (Fig. 3C). Under state $3_{+ADP}$ the steady-state $\Delta\Psi_m$ was, as expected, significantly lower than in state $4_{-ADP}$ ($176.8 \pm 2.2$ mV, $n = 19$, $P<0.05$ vs. the state $4_{-ADP}$-related $\Delta\Psi_m$). However, the difference in terms of calculated voltage was never larger than 20–25 mV. It can be noticed that, only at concentrations of KCN>50–100 μM does the state $3_{+ADP}$-related $\Delta\Psi_m$ start to decrease progressively, as for the state $4_{-ADP}$-related $\Delta\Psi_m$. However, at variance from this, the $\Delta\Psi_m$ maintained at values significantly higher, never dropping below 140 mV even at concentrations of the inhibitor suppressing the respiratory activity. The $\Delta\Psi_m$ is known to be generated, under certain

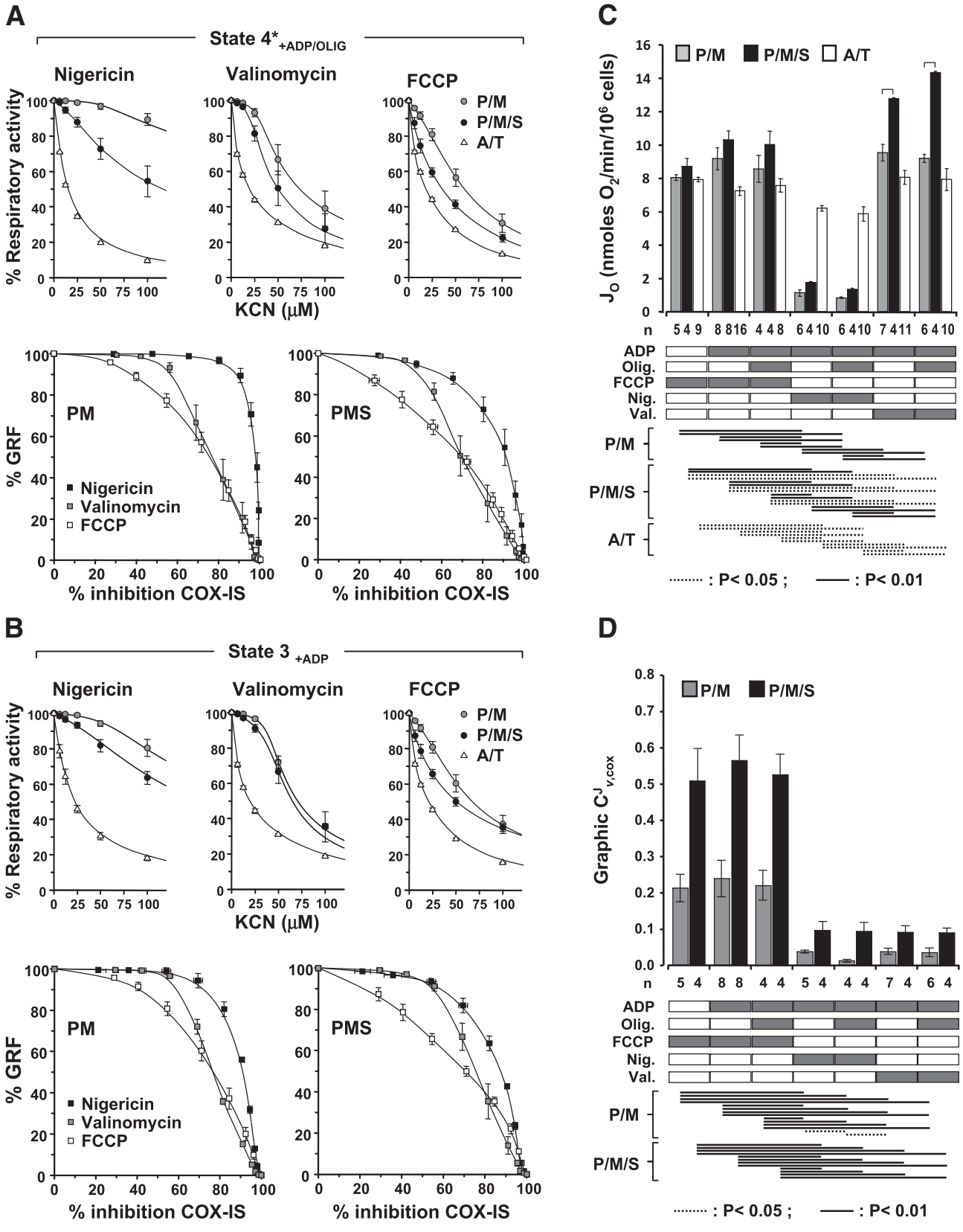


**Fig. 2.** Effect of ionophores on the inhibitory KCN titrations analysis of the respiratory activities in digitonin-permeabilized HepG2 cells. Permeabilized cells were preincubated 5 min before the addition of the respiratory substrates with either 35 nM nigericin or 45 nM valinomycin or 0.8 μM FCCP. Panels A and B, KCN titration performed in the presence of ADP + oligomycin (state $4^*_{+\,ADP\,+\,olig}$) or ADP alone (state $3_{+\,ADP}$) respectively using the respiratory substrate combinations as in Fig. 1 and indicated in the symbol legend. The tripartite upper part of the two panels shows the titrations at low concentration of KCN. Each point is the mean ± s.e.m. of $n \geq 5$ different cell preparations. The experimental data-sets for both the GRFs and the COX-ISs were best-fitted with a non-linear regression equation. The bipartite lower part of the two panels shows the threshold plot representations in the presence of each ionophore (as indicated in the symbol legends) and in the P/M- and P/M/S-dependent respiratory state. Panel C, uninhibited oxygen consumption rates of the GRF and COX-IS. Panel *D*, $C^J_{v,COX}$s measured by the "graphic" method. In C and D the presence of ADP, oligomycin and ionophores is indicated by the dark box; each bar indicates the mean value ± s.e.m. of the indicated *n* independent experiments; the statistical analysis between group-related pairs of values in panels is shown by connecting lines when the difference was significant.

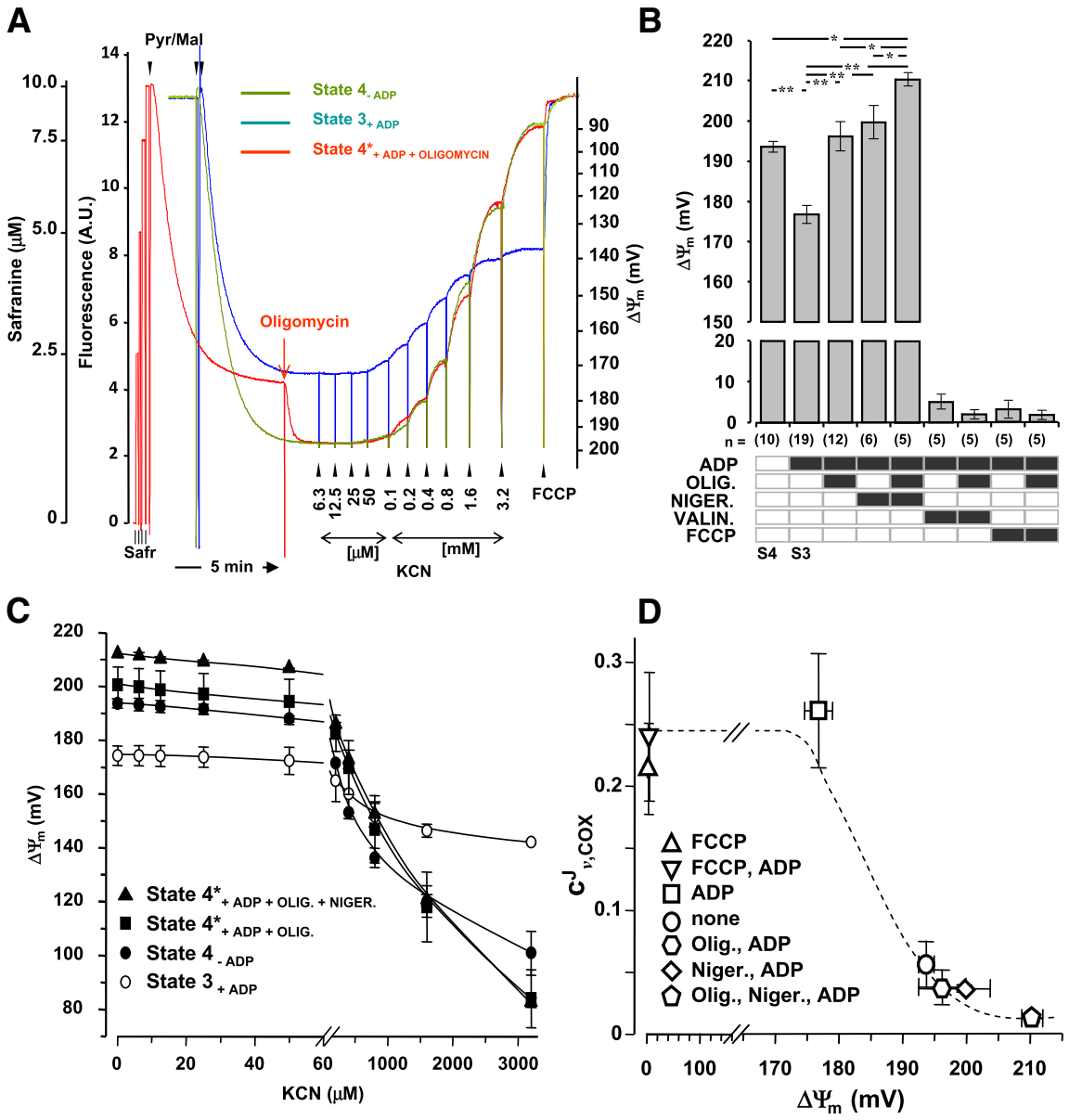


**Fig. 3.** Measurements of the $\Delta\Psi_m$ in digitonin-permeabilized HepG2 cells. Panel A, experimental traces of the spectrofluorimetric time-course recordings of the $\Delta\Psi_m$-related safranine O fluorescence changes. The experimental conditions are detailed in the Materials and Methods section. The three differently colored traces refer to the respiratory state conditions reported in the legend (i.e. ± 1 mM ADP). Where indicated the following additions were made: 2 mM pyruvate + 2 mM malate (Pyr/Mal), 1.25 μM oligomycin, and 0.8 μM FCCP. The final concentrations of KCN obtained by successive additions of the inhibitor are shown. The two left-sided y axes refer to the experimental fluorescence signal reported in arbitrary units (A.U.) and to the final concentration of safranine O calibrated by four successive additions of 2.5 μM of the fluorophore (in a non-linear scale). The right-sided y axis reports the calculated mitochondrial membrane potential (in a non-linear mV scale). Each trace is representative of 4–5 different experiments yielding similar results. Panel B, measured steady-state $\Delta\Psi_m$s attained under different respiratory state conditions with P/M used as respiratory substrates. When indicated 1.25 μM oligomycin, 1 mM ADP, 0.8 μM FCCP, 35 nM nigericin, and 45 nM valinomycin were present in the assay medium. S4 and S3 indicate the classical respiratory states $4_{-\,ADP}$ and $3_{+\,ADP}$ respectively. Each bar indicates the mean value ± s.e.m. of the indicated *n* independent experiments. The statistical analysis between pairs of $\Delta\Psi_m$ values is shown when the difference was significant. Panel C, effect of the KCN titration on the $\Delta\Psi_m$. The experimental conditions are those described in panel A and the different respiratory states tested are defined in the inset legend. Each point indicates the mean value ± s.e.m. of n ≥ 4 independent experiments. Panel D, relationship between the extent of the $\Delta\Psi_m$ and the $C^J_{v,COX}$. The $C^J_{v,COX}$s estimated by the "graphic" method (as reported in Figs. 1E, 2D) are plotted versus the steady-state $\Delta\Psi_m$ measured under identical P/M-sustained respiratory state conditions (as indicated in the symbol legend).

conditions, by the protonmotive activity of the $H^+$ FoF1 complex when functioning in the reverse ATP-ase instead of the ATP-synthase mode [23]. Addition of oligomycin together with ADP restored the sensitivity of the $\Delta\Psi_m$ to high concentration of KCN thereby indicating the occurrence under state $3_{+\,ADP}$ of a compensatory $H^+$ FoF1 ATP-ase-dependent outward protonmotive activity. Similar results were observed the P/M/S-"mode" of respiration (see Fig. S3). Importantly, when nigericin was present the measured $\Delta\Psi_m$ reached the value attained under state $4_{-\,ADP}$ even in the presence of ADP. In the presence of oligomycin, nigericin caused a further significant increase of the $\Delta\Psi_m$ with values as high as 210.3 ± 1.6 mV. Also in this case, the $\Delta\Psi_m$ started to be affected by the KCN titration al values higher than 50–100 μM.

The $\Delta\Psi_m$ generated by the protonmotive activity of the COX-IS did not show significant differences between states 4 and 3. Its extent was lower than that attained by the GRFs (i.e. ≈150 mV) and following KCN titration a significant decrease started to be detectable at concentrations of the inhibitor higher than 50–100 μM in a respiratory

state-independent manner (not shown). Both valinomycin and FCCP caused practically full prevention/collapse of both the GRF- and COX-IS-dependent $\Delta\Psi_m$.

These observations ruled out the possibility that the observed effect of the membrane energy state on the $C^J_{v,COX}$ was an artifact. The $C^J_{v,COX}$ was calculated by the inhibitory titration curve in the lowest concentration range of the KCN where no significant change of the $\Delta\Psi_m$ was in fact detectable. If some concern may be raised it regards the estimation of the "COX reserve capacity" which is calculated from data on the left side of the threshold plot [8]. Indeed, as shown in Fig. S4, an abrupt dissipation of the $\Delta\Psi_m$ takes place at the highest concentration of the inhibitor partially overlapping the decrease of the GRF at the same concentrations of KCN, in particular, for state(s) 4 and $3_{+\,ADP\,+\,NIG}$. Under these circumstances the effect of the membrane energy state cannot be unambiguously assessed as the inhibitory titration causes changes by itself in the $\Delta\Psi_m$.

Fig. 3D (see also Fig. S3) highlights the negative correlation occurring between the extent of the $\Delta\Psi_m$ and the value of the $C^J_{v,COX}$ estimated under the variety of the respiratory settings presented in this study.

It must be pointed out that the quantitative analysis presented here of the $\Delta\Psi_m$ relied on the estimation of the intracellular mitochondrial volume assessed by distribution of the membrane probe TMRE (see under Material and methods). This probe may not reliably provide a precise estimation of the matrix volume when used in conventional confocal microscopy. However, also if the value used in this study was overestimated it has to be considered that even halving the mitochondrial volume, the membrane potential would be scarcely affected because of the logarithmic relationship between the $\Delta\Psi_m$ and the distribution ratio of the probe. Moreover, quantification in mV of the $\Delta\Psi$ assessed by the safranine probe might lead to overestimation of the true absolute value. Indeed a $\Delta\Psi$-mediated binding of the probe to the membrane in addition to its partition between the two spaces of the dielectric cannot be excluded. Nevertheless, whatever was the real value of the $\Delta\Psi$ under state 4 of respiration the conclusion that its relative small decrease following transition to state 3 markedly affected $C^J_{v,COX}$ yet stands valid.

### *3.4. The membrane energy state exerts a similar effect on the respiratory flux control of complex I and complex III*

To verify whether the establishment of a large membrane potential influenced the $C^J_v$s of the other protonmotive RC complexes, the MCA was extended to the complexes I (NADH:UQ oxidoreductase) and III ($UQH_2$:cytochrome c oxidoreductase/bc1) titrating the GRF with the specific inhibitors rotenone and antimycin A respectively. Fig. 4A shows the inhibitor titration analysis of the P/M-sustained GRF with rotenone. Given the challenging technical difficulties in measuring the activity of the complex I-IS, only the inhibitory profiles of the GRF is reported. Under state $4_{-\,ADP}$ the respiratory activity was significantly more resistant to the inhibitory activity of rotenone as compared with that attained under state $3_{+\,ADP\,\pm\,FCCP}$. The $C^J_{v,CI}$ estimated by the "fitting" method resulted in: $0.124 \pm 0.002$, $0.448 \pm 0.024$, $0.531 \pm 0.189$ under states $4_{-\,ADP}$, $3_{+\,ADP}$, and $3^*_{+\,ADP\,+\,FCCP}$ respectively.

The MCA was also applied to complex III ($UQH_2$:cytochrome c oxidoreductase/$bc_1$) titrating with antimycin A the GRF. The results shown in Fig. 4B compare the inhibitory titration analysis of respiration under state $4^*_{+\,ADP/olig}$ and state $3_{+\,ADP}$ and unveil a complex sigmoidal profile. At relatively low concentrations of antimycin A the GRF was scarcely inhibited irrespective of the respiratory state. Beyond 10 nM of antimycin A the inhibition suddenly increased under state 3 whereas it was significantly more resistant under state 4. However, at 20–25 nM of antimycin A the respiration of both states 4 and 3 was practically zeroed. Antimycin A exhibits a very high affinity to complex III [24]. Thus, the titration, closely approaching the enzyme-inhibitor complex formation, indicated that the inhibitory action of antimycin A became significant when its concentration overcame the amount required to bind roughly half of the $bc_1$ molecules. The $bc_1$ complex is a homodimer [25] and evidences provided in literature show that electron transfer from ubiquinol to cytochrome c may occur via an inter-monomeric electron transfer mechanism when one of the two monomer is inhibited [26,27]. Therefore, the right shifted profile under state 3, starting at the semi-saturating concentration of antimycin A, might be an indication of the effect exerted by the $\Delta\Psi_m$ on the $C^J_v$ of the $bc_1$ dimer similarly to what was observed for complex I and COX. Although the MFC analysis of the antimycin A-titration curve was challenging we thought to remove the first part of the titration (roughly corresponding to 1:1 binding ratio of the inhibitor to the $bc_1$ homodimer) and to estimate the $C^J_v$ of complex III applying the fitting procedure to the residual normalized experimental points. Even in keeping the limitation of this approach the computed values of the $C^J_v$ was around 0.7 and 0.1 under state 3 and state 4 respectively.

The above-reported observations lead to the conclusion that the three protonmotive RC complexes (i.e. complex I, III and IV) share under condition of low membrane energization a larger control

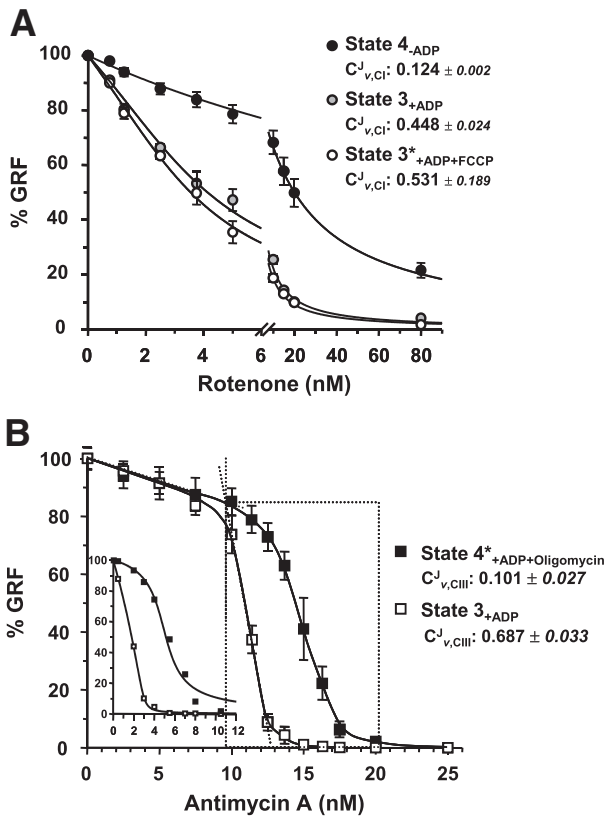


**Fig. 4.** Inhibitory titration analysis of the GRF by rotenone and antimycin A in digitonin-permeabilized HepG2 cells. Cells were permeabilized and assayed as described in the Materials and Methods section in the presence of 2 mM pyruvate + 2 mM malate. Panel A, effect of complex I-inhibition by rotenone on the GRF under states $4_{-\,ADP}$, $3_{+\,ADP}$ and $3^*_{+\,ADP/FCCP}$ (as indicated in the symbol legend); concentrations of ADP and FCCP were 1 mM and 0.8 μM respectively. Each point is the mean ± s.e.m. of n ≥ 5 different cell preparations. The experimental data-sets were best-fitted with the non-linear regression equation described in the Materials and Methods section and the estimated $C^J_{v,CI}$s (by the "fitting" method) reported. Panel B, effect of complex III-inhibition by antimycin A on the GRF under states $4^*_{+\,ADP/olig}$ and $3_{+\,ADP}$ (as indicated in the symbol legend). Each point is the mean ± s.e.m. of n ≥ 5 different cell preparations. The solid line fitting the experimental data-sets is from a routine polynomial equation. The inset shows the MFC analysis carried out on the inhibitory data sets devoid of the first titration points and normalized to the point intercepting the two linear slopes of the state $3_{+\,ADP}$-corresponding curve (see dotted square). The residual points were analyzed by the "fitting" procedure and the computed $C^J_{v,CIII}$ shown.

strength over respiration as compared to that exerted under high membrane energization settings.

## 4. Discussion

### 4.1. The MCA supports the occurrence of mitochondrial RC supercomplexes

The effect of the $\Delta\mu_{H+}$ in controlling the actual rate of electron transfer in the mitochondrial RC is long known and constitutes the basis of the respiratory control adapting the $O_2$ consumption rate to the cellular energy demand [1,17]. In this study we applied the MCA to investigate the impact of the protonmotive force on the control strength exerted by the RC complexes on the GRF. The main results attained and our interpretation thereof are given point by point in the following.

The results shown in Fig. 1 indicate that the quantitative estimation of the $C^J_{v,COX}$ depends on the combination of the respiratory substrates used. The explanation that we offer to rationalize this observation relies on and is consistent with the notion that the mitochondrial RC is organized in discrete multi-complex units (defined supercomplexes or respirosomes) [28,29] functionally depending on the reducing substrate initiating the electron transfer.

Since a given respiratory substrate will select/activate specific RC multicomplex units this introduces some caveats in the interpretation of the inhibitor titration assay used to calculate the $C^J_v$ according to the MCA. In particular, a lower inhibition of the GRF, as compared with that attainable with the IS at the same concentration of the inhibitor, is expected. Because cyanide binds to all the COX molecules irrespectively of the unit where COX is present there will be, under conditions where not all the multicomplex units are active, a subset of COX molecules buffering the effect of the inhibitor when the GRF is titrated with cyanide. When the choice of substrates used is such that more RC multi-complex units are recruited the artifactual inhibitor-buffering effect of the isolated step is reduced (see the scheme in Fig. S5).

It can be noted that when the respiratory substrate used is the sole succinate the $C^J_{v,COX}$ is relatively low (Fig. 1C). A plausible explanation for this observation is that complex II does not participate to formation of any RC-supercomplex (consistent with [30,31]) and this will introduce upstream of COX a kinetic limiting factor strongly reducing the $C^J_{v,COX}$. Our observations are consistent with the occurrence in vivo of the following prominent RC-units: $^{NADH}RC_{[CI,CIII,CIV)}$ and $^{Succ\text{-}CII}RC_{[CIII,CIV)}$, where the subscript indicates the composition of the supercomplex and the superscript indicates the reducing substrate/complex. An alternative explanation is that complex II is recruited to form the supercomplex $^{NADH/Succ}RC_{[CI,CII,CIII,CIV]}$ when complex I is functionally active.

The occurrence of RC supercomplexes is further functionally supported by the observation that all the three protonmotive RC complexes (i.e. complex I, III and IV) share under condition of low membrane energization a large control strength over respiration (Fig. 4). The metabolic control theory foresees that the sum of the control coefficients of the enzymatic steps within a given pathway cannot exceed the value of unity unless a number of steps organize in multi-enzymatic structural/functional units [2–4,31]. In this study we show that the control coefficients of COX and complex I resulted under de-energized conditions in values which when summed approached the limiting value of unity. Considering also the tentative estimates of the $C^J_v$ of complex III and the possibility that the $C^J_v$s of the RC complexes in permeabilized cells may result slightly lower than under in vivo conditions (i.e. in intact cells) the limiting value foreseen by the MCA may well be overcome.

It must be pointed out that the effect of the respiratory substrate combination on the $C^J_{v,COX}$ is more evident under state $3_{+ADP}$ (see ahead in the Discussion for a comprehensive explanation). However, irrespective of the combination of respiratory substrate used (with the exception of succinate alone) the $C^J_{v,COX}$ under state(s) 4 of respiration proved to be much lower than under state 3.

The results shown in Figs. 2 and 3 unveil that the establishment of a large $\Delta\Psi_m$ and/or $\Delta pH_m$ causes a decrease of the $C^J_{v,COX}$. However, the two components of the $\Delta\mu_{H+}$, although thermodynamically equivalent, did not sum up their relative effects. This is highlighted by the effect elicited by both nigericin and valinomycin when added to the respiratory state $3_{+ADP}$. Thus, to exert the depressing effect on the $C^J_{v,COX}$ both the $\Delta\Psi_m$ and the $\Delta pH_m$ need to overcome some specific threshold value whereas a thermodynamic summation of sub-threshold values of the two $\Delta\mu_{H+}$ components is apparently ineffective. This leads to the conclusion that the action of the $\Delta\Psi_m$ and of the $\Delta pH_m$ actuates by a different mechanism. Evidently, the establishment of both a large $\Delta\Psi_m$ and $\Delta pH_m$ unleashes the respiratory control strength of COX attained under uncoupled or state 3 respiration and places the main kinetic limitation(s) somewhere (or somehow) upstream of COX. A schematic view of this concept is provided in Fig. 5.

It must be pointed out, however, that the control exerted by the $\Delta pH_m$ is unlikely to play a role of physiological relevance. Indeed establishment of very large $\Delta pH_m$ has never been documented under in vivo conditions. Conversely, variations of the $\Delta\Psi_m$ following the state 4 to state 3 transition and vice versa are likely to occur in consequence of changes of the energy demand of the cell.

In a recent MCA-study on intact HepG2, Dalmonte et al. [10] reported similarly to our results that the $C^J_{v,COX}$ estimated in the presence of valinomycin was significantly reduced as compared with that estimated under either resting (i.e. a state 3-like condition) and uncoupled conditions. However, conflicting with our results nigericin did not change the $C^J_{v,COX}$ exhibiting values as high as that measured under resting or uncoupled conditions. In this study the authors did not measure directly the effect of nigericin on the $\Delta\Psi_m$, as we did, taking for granted a full conversion of the $\Delta\mu_{H+}$ in $\Delta\Psi_m$. Fig. S6 shows that relatively higher concentration of nigericin with respect to that utilized in our study resulted in a paradoxical progressive reduction of the $\Delta\Psi_m$ likely due to the protonophoric property of nigericin which under certain conditions may overcome its $K^+/H^+$ exchange activity. It is plausible that, at the relatively high concentration of nigericin used in [10] (i.e. three-fold higher then that assessed to be optimal in our study) a condition was settled where the actual $\Delta\Psi_m$ was comparable if not lower than that attained under resting respiration thus precluding to assess the real depressing effect of a high $\Delta\Psi_m$ on the $C^J_{v,COX}$.

The summation corollary of the metabolic control theory foresees that a decrease in the $C^J_v$ of a given enzymatic step may arise from the introduction in the pathway of one or more additional step(s) [2]. It is largely documented that at high protonmotive force (like that elicited by the presence of oligomycin) the mitochondrial respiratory rate is dominated by the proton suck-back (proton leak) across the membrane [32, see also 33]. Although this notion is phenomenologically undisputable nevertheless it has nothing to do with the conclusions drawn from our observations. Indeed, the establishment of a large FCCP-mediated proton leak across the membrane results in a $C^J_{v,COX}$ undistinguishable from that estimated under state 3 of respiration in spite of the fact that a new step in the integrated metabolic pathway has been "introduced".

Furthermore, the experiment on valinomycin-treated cells presented in Fig. 2 shows that substitution of the transmembrane electrical potential with a pH gradient resulted in no change in COX control. Given the large difference in membrane conductivity of protons with respect to other cations or anions (the membrane conductance for $H^+$ is at least $10^6$ times higher than for $K^+$ [34]), one would expect a tighter control of $\Delta pH$ in the metabolic network and, as a consequence, a compensatory decrease of the control coefficients of the other steps. In addition the non-Ohmic flow–force relationship, which is a measure of the proton leak, is known to vanish when the

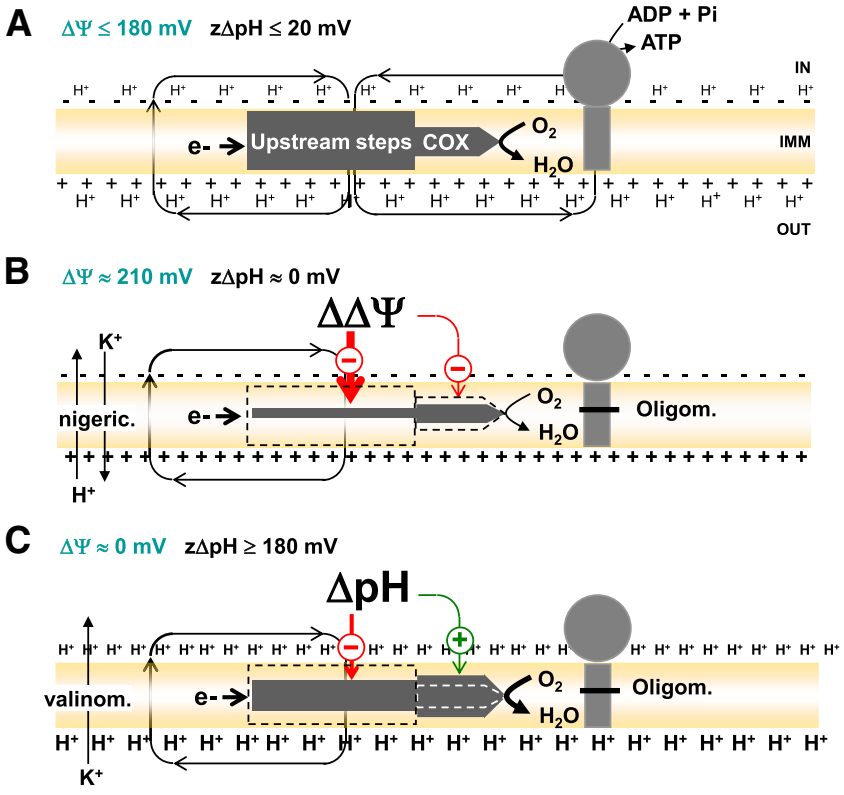


**Fig. 5.** Proposed model for the effect of the two components of the $\Delta\mu_{H+}$, $\Delta\Psi_m$ and $\Delta pH_m$, on the controlling step(s) in the RC activity. Three thermodynamic conditions are schematically indicated, distinguished either by the presence of a relatively low $\Delta\mu_{H+}$ (A) or by the presence of each or the other of its two components $\Delta\Psi_m$ (B) or $\Delta pH_m$ (C) at their maximal attainable steady-state value (i.e. in the presence of nigericin or valinomycin respectively and with the $H^+$ FoF1 ATP synthase blocked by oligomycin). The respiratory chain is schematized as a bipartite dark box within the mitochondrial membrane with a part constituted by the COX and the other by all the steps located upstream. To visualize the mechanism of control on the GRF the thickness of the bipartite box is inversely correlated with the control strength exerted by that part of the RC. Note that the thickness of the "$O_2 \rightarrow H_2O$" arrow reflects the GRF-activity shown in Figs. 1D and 2C. In the presence of a relatively low $\Delta\mu_{H+}$ (either with an uncoupler (not shown) or under state 3 respiration (shown), panel A) COX exhibits a large $C^J_{v,COX}$ over the cellular $O_2$ consumption with a relatively low reserve capacity. The establishment of a large $\Delta\Psi_m$ (panel B) causes a marked depression of the global oxygen consumption rate and shifts the major control strength to step(s) upstream of COX. When a full $\Delta pH_m$ establishes (panel C) the overall metabolic flux is comparable with that of the uncoupled respiration or state $3_{+ADP}$ but the $C^J_{v,COX}$ of COX is again relatively lowered. Also in this case the $\Delta pH_m$ affects differently the capacities of the RC-related steps with the one acquiring the more stringent control strength located upstream of COX.

electrical gradient is substituted with a pH gradient [35]. Thus, a high $\Delta\Psi$ or $\Delta pH$ exert the same phenomenological effect on the COX-dependent flux control independently on the proton leak.

Moreover, the "flow–force" plotting of the respiratory rates of the states $4_{-ADP}$- and $4^*_{+ADP+olig}$-dependent GRFs as a function of the respective $\Delta\Psi_m$ demonstrated that the non-Ohmic degree of dependence of the proton leak on the $\Delta\Psi_m$ resulted to be lower when the $\Delta\Psi_m$ was "clamped" in the presence of the $H^+$ FoF1-ATP synthase inhibitor (Fig. S7). This indicated that the utilization of oligomycin to establish a large $\Delta\Psi_m$ did not introduce further steps in the control of the GRF as compared to the more physiological state $4_{-ADP}$.

Therefore, in our opinion, the proton leak controls indirectly the overall respiration by setting the actual value of the $\Delta\Psi_m$, which in turn controls directly the distribution of the control strengths within the different enzymatic steps constituting the respiratory pathway. It is worth noting that the $\Delta\Psi_m$ range where the depressing effect on the $C^J_{v,cox}$ was observed (i.e. between 170 and 210 mV) closely overlapped that where the change in the membrane proton conductivity is more evident (cf. Figs. 3D and S7 and see ahead in the Discussion).

The results so far discussed might apparently recall those reported by our group in an earlier publication [9]. However, it must be pointed out that further substantial new observations are provided in the present study as outlined in the following. (a) Tissue variation in the control coefficient distribution of the OXPHOS complexes has been reported [6,36] under state $3_{+ADP}$. Here we show that the lowering of the $C^J_{v,cox}$ under conditions preserving dissipation of the $\Delta\mu_{H+}$ in endogenously respiring intact HepG2 cells [9] was confirmed in intact murine myoblasts (L6) cell line and primary normal human dermal fibroblasts (NDHF) (Fig. S1) thereby indicating that the depressing effect of the mitochondrial protonmotive force on the $C^J_{v,cox}$ is a physiological relevant phenomenon irrespective of the cell phenotypical background. (b) The combination of selected respiratory substrates enabled to differentiate the impact of the membrane energy state on the $C^J_{v,cox}$ as a function of the involved RC complexes. (c) The MCA was extended to the RC complexes III and IV unveiling on a semiquantitative basis an effect of the respiratory states on the $C^J_v$s similar to that observed for COX. (d) Finally, and most relevant, the quantitative estimation of the voltage gradients in the different respiratory states unveiled that the decrease of the $C^J_{v,cox}$ was not a linear function of the $\Delta\Psi_m$ amplitude but instead an "all or none" response over a critical voltage-threshold value. Obviously, the mechanistic implications of this last observation must be taken into account to explain the mode of action.

Permeabilization of the cell membrane causes dilution of cytosolic metabolites which may exert regulatory functions on the mitochondrial RC. In particular the intra- and extra-mitochondrial ATP/ADP ratio appears to be a an important controller of the COX activity [37,38], with a high ATP/ADP ratio inhibiting the activity of COX in an allosteric mode. Moreover, recently it has been shown that the ATP-mediated allosteric inhibition of COX requires a cAMP-dependent

phosphorylation of COX [39]. However, a direct effect of externally added ADP (i.e. low cytosolic ATP/ADP ratio) on the increased $C^J_{v,COX}$ under state 4 of respiration has to be ruled out because in the presence of oligomycin + ADP a decrease of $C^J_{v,COX}$ was observed. As we cannot exclude alterations of the allosteric effect of matrix ATP the observations reported in this study might concern an intrinsic feature of the respiratory chain irrespective of a second respiratory control "mode" [40]. However, it must be noted that both in intact and permeabilized HepG2 cells the $C^J_{v,COX}$ resulted in comparable values under state 3 of respiration and decreased by the same extent following transition to state 4. Moreover, our results suggest that the membrane potential-dependent change of the flux control coefficient apply not only to COX but also to the other two protonmotive complexes of the RC, for which a regulatory role exerted by the adenine nucleotides has not been demonstrated.

In the attempt to rationalize the reported observations we offer a model which, although not supported by direct physical evidence, nevertheless might be taken in account as a working hypothesis susceptible to experimental validation. It is proposed that the mitochondrial RC complexes exist in two states, as single molecular units or as supramolecular complexes. The two states are in dynamic equilibrium and the electrical transmembrane potential beyond/below a critical threshold value controls the equilibrium and the occupancy of a given RC complex in one or the other of the two states (see Fig. S8). The stoichiometry of the complexes in the aggregated state is variable but driven by specific protein–protein interactions. Under condition of absent or relatively low $\Delta\Psi_m$ (<180 mV) the aggregation state is favored whereas at higher voltage (210–220 mV) the polydisperse state of the RC complexes prevails. This model is consistent with the results presented in this study. Indeed, the supercomplex state will confer high kinetic efficiency in terms of electron transfer as the local availability of the reduced substrates/metabolites is not limiting [41].

As a consequence, the supercomplex will behave as a functional unit with high $C^J_v$s pertaining to the single complexes that when summed will result in a value approaching or even overcoming the theoretical limit of unity. Under this condition the reserve capacity of the respiratory chain will be low and any change in each or the other of the enzymatic steps constituting the complex will cause an almost proportional change in the GRF. Under the polydisperse state each enzymatic step will behave separately and their functional connectivity will strongly depend on one hand from the collisional rate constants of the isolated complex and of their electron donating/accepting substrates [42] and on the other hand from the differential effect exerted by the voltage gradient on the intrinsic electrogenic steps of each or the other of the RC complexes [1,43,44]. This is expected to slow down the global respiratory flux, to decrease the $C^J_v$s of the enzymatic steps and to enhance the functional reserve capacity of the RC complexes.

How the change in the structural assembly of the RC complexes is achieved by the small increment of the $\Delta\Psi_m$ was out of the scope of this study. However, a number of possibilities can be envisaged and experimentally assessed/scrutinized. Some physical–chemical features of the phospholipid bilayer proved to be affected by the establishment of a voltage transmembrane gradient. For instance the (micro)viscosity of the membrane was found to vary as an exponential function of an applied potential with a sharp increase beyond 180 mV [45,46]. If we consider the actual structure of the RC complexes as resulting from a dynamic equilibrium between the supercomplexes and their isolated units it is plausible to hypothesize that an enhanced membrane viscosity would favor the occupancy of the complexes in the isolated state limiting their diffusion-controlled interactions.

Thus in addition to the recognized role of the energy charge (modulating the activity of the $H^+$ FoF1 ATP synthase), of the $\Delta\mu_{H+}$ (modulating the rates of electrogenic steps) and of the allosteric/covalent regulation (modulating the activity of the RC-complexes) our model provides a further additional insight to the mechanism of the respiratory control adapting the respiratory activity of the RC to the changing cellular energy requirement.

## Acknowledgements

The work was supported by the University of Foggia (Local Research Funds 2005–2008). The authors have no financial or other conflict of interest related to this study. N.C. wishes to acknowledge Dr. Gaetano Villani (University of Bari) for his stimulating criticism on issues related to this study.

## Appendix A. Supplementary data

Supplementary data to this article can be found online at doi:10.1016/j.bbabio.2011.04.001.

## References

[1] D.G. Nicholls, S.J. Ferguson, Bioenergetics, 3 rd ed. Academic Press, London, 2002.
[2] A. Kacser, J.A. Burns, The control of flux, Symp. Soc. Exp. Biol. 32 (1973) 65–104.
[3] R. Heinrich, T.A. Rapoport, A linear steady-state treatment of enzymatic chains. Critique of the crossover theorem and a general procedure to identify interaction sites with an effector, Eur. J. Biochem. 42 (1974) 97–105.
[4] C. Reder, Metabolic control theory: a structural approach, J. Theor. Biol. 135 (1988) 175–201.
[5] J.P. Mazat, T. Letellier, F. Bédes, M. Malgat, B. Korzeniewski, L.S. Jouaville, R. Morkuniene, Metabolic control analysis and threshold effect in oxidative phosphorylation: implications for mitochondrial pathologies, Mol. Cell. Biochem. 174 (1997) 143–148.
[6] R. Rossignol, M. Malgat, J.P. Mazat, T. Letellier, Threshold effect and tissue specificity. Implication for mitochondrial cytopathies, J. Biol. Chem. 274 (1999) 33426–33432.
[7] G.C. Brown, Control of respiration and ATP synthesis in mammalian mitochondria and cells, Biochem. J. 284 (1992) 1–13.
[8] G. Villani, G. Attardi, In vivo control of respiration by cytochrome c oxidase in wild-type and mitochondrial DNA mutation-carrying human cells, Proc. Natl. Acad. Sci. 94 (1997) 1166–1171.
[9] C. Piccoli, R. Scrima, B. Boffoli, N. Capitanio, Control by cytochrome c oxidase of the cellular oxidative phosphorylation system depends on the mitochondrial energy state, Biochem. J. 396 (2006) 573–583.
[10] M.E. Dalmonte, E. Forte, M.L. Genova, A. Giuffrè, P. Sarti, G. Lenaz, Control of respiration by cytochrome c oxidase in intact cells: role of the membrane potential, J. Biol. Chem. 284 (2009) 32331–32335.
[11] F.N. Gellerich, W.S. Kunz, R. Bohnensack, Estimation of flux control coefficients from inhibitor titrations by non-linear regression, FEBS Lett. 274 (1990) 167–170.
[12] J.R. Small, Flux control coefficients determined by inhibitor titration: the design and analysis of experiments to minimize errors, Biochem. J. 296 (1993) 423–433.
[13] K.E. Akerman, M.K. Wikström, Safranine as a probe of the mitochondrial membrane potential, FEBS Lett. 68 (1976) 191–197.
[14] L.V. Johnson, M.L. Walsh, B.J. Bockus, L.B. Chen, Monitoring of relative mitochondrial membrane potential in living cells by fluorescence microscopy, J. Cell Biol. 88 (1981) 526–535.
[15] P. Lund, D. Wiggins, The matrix water space of mitochondria in situ in isolated hepatocytes, Biosci. Rep. 7 (1987) 59–66.
[16] M. Pinti, L. Troiano, M. Nasi, R. Ferraresi, J. Dobrucki, A. Cossarizza, Hepatoma HepG2 cells as a model for in vitro studies on mitochondrial toxicity of antiviral drugs: which correlation with the patient? J. Biol. Regul. Homeost. Agents 17 (2003) 166–171.
[17] B. Chance, G.R. Williams, Respiratory enzymes in oxidative phosphorylation. III. The steady state, J. Biol. Chem. 217 (1955) 409–427.
[18] M.T. Wilson, G. Antonini, F. Malatesta, P. Sarti, M. Brunori, Probing the oxygen binding site of cytochrome c oxidase by cyanide, J. Biol. Chem. 269 (1994) 24114–24119.
[19] C.E. Cooper, G.C. Brown, The inhibition of mitochondrial cytochrome oxidase by the gases carbon monoxide, nitric oxide, hydrogen cyanide and hydrogen sulfide: chemical mechanism and physiological significance, J. Bioenerg. Biomembr. 40 (2008) 533–539.
[20] N. Capitanio, E. De Nitto, G. Villani, G. Capitanio, S. Papa, Protonmotive activity of cytochrome c oxidase: control of oxidoreduction of the heme centers by the protonmotive force in the reconstituted beef heart enzyme, Biochemistry 29 (1990) 2939–2945.
[21] T. Tsukihara, H. Aoyama, E. Yamashita, T. Tomizaki, H. Yamaguchi, K. Shinzawa-Itoh, R. Nakashima, R. Yaono, S. Yoshikawa, Structures of metal sites of oxidized bovine heart cytochrome c oxidase at 2.8 A, Science 269 (1995) 1069–1074.
[22] L.B. Chen, Mitochondrial membrane potential in living cells, Annu. Rev. Cell Biol. 4 (1988) 155–181.
[23] M. Dittrich, S. Hayashi, K. Schulten, On the mechanism of ATP hydrolysis in F1-ATPase, Biophys. J. 85 (2003) 2253–2266.

[24] G. von Jagow, T.A. Link, Use of specific inhibitors on the mitochondrial bc1 complex, Methods Enzymol. 126 (1986) 253–271.
[25] D. Xia, C.A. Yu, H. Kim, J.Z. Xia, A.M. Kachurin, L. Zhang, L. Yu, J. Deisenhofer, Crystal structure of the cytochrome bc1 complex from bovine heart mitochondria, Science 277 (1997) 60–66.
[26] G. Bechmann, H. Weiss, P.R. Rich, Non-linear inhibition curves for tight-binding inhibitors of dimeric ubiquinol-cytochrome c oxidoreductases. Evidence for rapid inhibitor mobility, Eur. J. Biochem. 208 (1992) 315–325.
[27] M. Castellani, R. Covian, T. Kleinschroth, O. Anderka, B. Ludwig, B.L. Trumpower, Direct demonstration of half-of-the-sites reactivity in the dimeric cytochrome bc1 complex: enzyme with one inactive monomer is fully active but unable to activate the second ubiquinol oxidation site in response to ligand binding at the ubiquinone reduction site, J. Biol. Chem. 285 (2010) 502–510.
[28] N.V. Dudkina, S. Sunderhaus, E.J. Boekema, H.P. Braun, The higher level of organization of the oxidative phosphorylation system: mitochondrial supercomplexes, J. Bioenerg. Biomembr. 40 (2008) 419–424.
[29] J. Vonck, E. Schäfer, Supramolecular organization of protein complexes in the mitochondrial inner membrane, Biochim. Biophys. Acta 1793 (2009) 117–124.
[30] W.S. Kunz, A. Kudin, S. Vielhaber, C.E. Elger, G. Attardi, G. Villani, Flux control of cytochrome c oxidase in human skeletal muscle, J. Biol. Chem. 275 (2000) 27741–27745.
[31] C. Bianchi, M.L. Genova, G. Parenti Castelli, G. Lenaz, The mitochondrial respiratory chain is partially organized in a supercomplex assembly: kinetic evidence using flux control analysis, J. Biol. Chem. 279 (2004) 36562–36569.
[32] M.D. Brand, R.P. Hafner, G.C. Brown, Control of respiration in non-phosphorylating mitochondria is shared between the proton leak and the respiratory chain, Biochem. J. 255 (1988) 535–539.
[33] A.K. Groen, R.J.A. Wanders, H.V. Westerhoff, R. Van der Meer, J.M. Tager, Quantification of the contribution of various steps to the control of mitochondrial respiration, J. Biol. Chem. 257 (1982) 2754–2757.
[34] J.M. Wrigglesworth, C.E. Cooper, M.A. Sharpe, P. Nicholls, The proteoliposomal steady state. Effect of size, capacitance and membrane permeability on cytochrome-oxidase-induced ion gradients, Biochem. J. 270 (1990) 109–118.
[35] G. Krishnamoorty, P.C. Hinckle, Non-Ohmic proton conductance of mitochondria and liposomes, Biochemistry 231 (1984) 1640–1645.
[36] R. Rossignol, T. Letellier, M. Malgat, C. Rocher, J.P. Mazat, Tissue variation in the control of oxidative phosphorylation: implication for mitochondrial diseases, Biochem. J. 347 (2000) 45–53.
[37] J. Napiwotzki, B. Kadenbach, Extramitochondrial ATP/ADP-ratios regulate cytochrome c oxidase activity via binding to the cytosolic domain of subunit IV, Biol. Chem. 379 (1998) 335–339.
[38] S. Arnold, B. Kadenbach, Cell respiration is controlled by ATP, an allosteric inhibitor of cytochrome-c oxidase, Eur. J. Biochem. 249 (1997) 350–354.
[39] S. Helling, S. Vogt, A. Rhiel, R. Ramzan, L. Wen, K. Marcus, B. Kadenbach, Phosphorylation and kinetics of mammalian cytochrome c oxidase, Mol. Cell. Proteomics 7 (2009) 1714–1724.
[40] B. Kadenbach, R. Ramzan, L. Wen, S. Vog, New extension of the Mitchell Theory for oxidative phosphorylation in mitochondria of living organisms, Biochim. Biophys. Acta 1800 (2010) 205–212.
[41] E. Schäfer, N.A. Dencher, J. Vonck, D.N. Parcej, Three-dimensional structure of the respiratory chain supercomplex I1III2IV1 from bovine heart mitochondria, Biochemistry 46 (2007) 12579–12585.
[42] G. Lenaz, A. Baracca, G. Barbero, C. Bergamini, M.E. Dalmonte, M. Del Sole, M. Faccioli, A. Falasca, R. Fato, M.L. Genova, G. Sgarbi, G. Solaini, Mitochondrial respiratory chain super-complex I–III in physiology and pathology, Biochim. Biophys. Acta 1797 (2010) 633–640.
[43] P.R. Rich, The osmochemistry of electron-transfer complexes, Biosci. Rep. 11 (1991) 539–568.
[44] S. Papa, M. Lorusso, N. Capitanio, Mechanistic and phenomenological features of proton pumps in the respiratory chain of mitochondria, J. Bioenerg. Biomembr. 26 (1994) 609–618.
[45] D. Corda, C. Pasternak, M. Shinitzky, Increase in lipid microviscosity of unilamellar vesicles upon the creation of transmembrane potential, J. Membr. Biol. 65 (1982) 235–242.
[46] P.S. O'Shea, S. Feuerstein-Thelen, A. Azzi, Membrane-potential-dependent changes of the lipid microviscosity of mitochondria and phospholipid vesicles, Biochem. J. 220 (1984) 795–801.